






# Ex vivo Ikk $\beta$ ablation rescues the immunopotency of mesenchymal stromal cells from diabetics with advanced atherosclerosis

Ozge Kizilay Mancini<sup>1</sup>, David N. Huynh <sup>1</sup>, Liliane Menard <sup>1</sup>,  
Dominique Shum-Tim <sup>2,3</sup>, Huy Ong<sup>1</sup>, Sylvie Marleau <sup>1</sup>, Ines Colmegna<sup>4</sup>, and  
Marc J. Servant <sup>1,5\*</sup>

<sup>1</sup>Faculty of Pharmacy, University of Montreal, C.P. 6128, Succursale Centre-Ville, Montréal, QC H3C 3J7, Canada; <sup>2</sup>Division of Cardiac Surgery Department of Surgery, McGill University, Montreal, QC H4A 3J1, Canada; <sup>3</sup>Division of Surgical Research, Department of Surgery, McGill University, Montreal, QC H4A 3J1, Canada; <sup>4</sup>Division of Rheumatology, Department of Medicine, McGill University, Montreal, QC H4A 3J1, Canada; and <sup>5</sup>Réseau Québécois de Recherche sur les Médicaments Centre de recherche, CHU Sainte-Justine 3175 Chemin de la Côte-Ste-Catherine Montréal, QC H3T 1C5, Canada

Received 25 March 2020; revised 16 April 2020; editorial decision 20 April 2020; accepted 21 April 2020; online publish-ahead-of-print 1 July 2020

**Time for primary review: 9 days**

## Aims

Diabetes is a conventional risk factor for atherosclerotic cardiovascular disease and myocardial infarction (MI) is the most common cause of death among these patients. Mesenchymal stromal cells (MSCs) in patients with type 2 diabetes mellitus (T2DM) and atherosclerosis have impaired ability to suppress activated T-cells (i.e. reduced immunopotency). This is mediated by an inflammatory shift in MSC-secreted soluble factors (i.e. pro-inflammatory secretome) and can contribute to the reduced therapeutic effects of autologous T2DM and atherosclerosis-MSC post-MI. The signalling pathways driving the altered secretome of atherosclerosis- and T2DM-MSC are unknown. Specifically, the effect of I $\kappa$ B kinase  $\beta$  (IKK $\beta$ ) modulation, a key regulator of inflammatory responses, on the immunopotency of MSCs from T2DM patients with advanced atherosclerosis has not been studied.

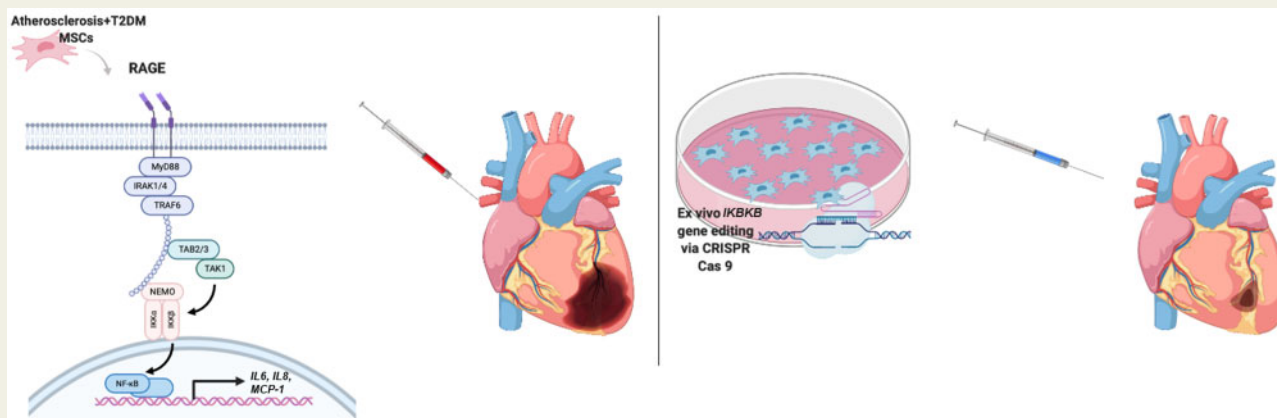
## Methods and results

MSCs were isolated from adipose tissue obtained from patients with (i) atherosclerosis and T2DM (atherosclerosis+T2DM MSCs,  $n = 17$ ) and (ii) atherosclerosis without T2DM (atherosclerosis MSCs,  $n = 17$ ). MSCs from atherosclerosis+T2DM individuals displayed an inflammatory senescent phenotype and constitutively expressed active forms of effectors of the canonical IKK $\beta$  nuclear factor- $\kappa$ B transcription factors inflammatory pathway. Importantly, this constitutive pro-inflammatory IKK $\beta$  signature resulted in an altered secretome and impaired *in vitro* immunopotency and *in vivo* healing capacity in an acute MI model. Notably, treatment with a selective IKK $\beta$  inhibitor or IKK $\beta$  knockdown (KD) (clustered regularly interspaced short palindromic repeats/Cas9-mediated IKK $\beta$  KD) in atherosclerosis+T2DM MSCs reduced the production of pro-inflammatory secretome, increased survival, and rescued their immunopotency both *in vitro* and *in vivo*.

## Conclusions

Constitutively active IKK $\beta$  reduces the immunopotency of atherosclerosis+T2DM MSC by changing their secretome composition. Modulation of IKK $\beta$  in atherosclerosis+T2DM MSCs enhances their myocardial repair ability.

## Graphical Abstract



**Keywords** Mesenchymal stromal cells • Immunopotency • IKK beta signalling • Inflammation

## 1. Introduction

Type 2 diabetes mellitus (T2DM) is a major risk factor for atherosclerosis. Patients with T2DM develop severe and extensive atherosclerosis almost two decades earlier than people without T2DM.<sup>1</sup> T2DM promotes the inflammatory state that contributes to atherosclerotic lesion initiation and plaque rupture.<sup>2</sup> Accumulation of senescent cells contributes to inflammatory state through the secretion of pro-inflammatory cytokines, chemokines, and growth factors, known as senescence-associated secretory phenotype (SASP) or senescence-messaging secretome.<sup>3,4</sup> The production of SASP is mediated by I $\kappa$ B kinase  $\beta$  (IKK $\beta$ ) through the activation of nuclear factor- $\kappa$ B transcription factors (NF- $\kappa$ B).<sup>5</sup>

The NF- $\kappa$ B family comprises five members: p65 (RelA), RelB, c-Rel, p100/p52, and p105/p50. Under basal conditions NF- $\kappa$ B transcription factors are bound to inhibitor of  $\kappa$ B (I $\kappa$ B) proteins within the cytoplasm. Cellular insults including reactive oxygen species (ROS), DNA damage, or pro-inflammatory cytokines activate the IKK complex which induces I $\kappa$ Bs phosphorylation-dependent turnover. Degradation of I $\kappa$ Bs releases NF- $\kappa$ B dimers, which can in turn translocate into the nucleus to initiate transcription of target genes. The IKK complex involves two kinase subunits, namely IKK $\alpha$  and IKK $\beta$ , and the regulatory subunit NF- $\kappa$ B essential modulator (NEMO, or IKK $\gamma$ ).<sup>6</sup> Canonical activation of NF- $\kappa$ B and its downstream target genes requires the IKK $\beta$  catalytic subunit. Activation of IKK $\beta$ -mediated NF- $\kappa$ B is implicated in the pathogenesis of atherosclerosis.<sup>7</sup> Activated IKK $\beta$ -NF- $\kappa$ B axis is observed in endothelial cells, macrophages, and smooth muscle cells from human atherosclerotic plaques and is upregulated in unstable plaques.<sup>8</sup> Myeloid cell-specific deletion of IKK $\beta$  reduces atherosclerotic lesions and insulin resistance in murine models by attenuating macrophage inflammatory gene expression, adhesion, migration, and lipid uptake.<sup>9</sup> Genetic inhibition of several IKK $\beta$ -NF- $\kappa$ B target genes, including vascular cell adhesion molecule-1, intercellular adhesion molecule-1, E- and P-selectins, tumour necrosis factor- $\alpha$ , and interleukin (IL)-1 $\beta$  also interferes with atherosclerotic lesion formation.<sup>10</sup> Due to the extensive evidence supporting the role of inflammation in the aetiology and pathophysiology of accelerated atherosclerosis in T2DM, several clinical trials evaluate the therapeutic effects of

targeting inflammation (reviewed in Ref.11). These studies provide a proof-of-concept that modulation of inflammatory pathways result in cardiovascular risk reduction especially in high-risk groups such as T2DM. However, the magnitude of improvement is relatively modest when a single cytokine is targeted.<sup>12</sup> This emphasizes the potential relevance of approaches targeting multiple inflammatory mechanisms.

Mesenchymal stromal cells (MSCs) are multipotent tissue-resident cells. MSCs migrate to inflammatory zones where they promote immune tolerance. MSCs therapy is being tested for a variety of inflammatory and autoimmune conditions including atherosclerosis and T2DM.<sup>13</sup> In murine atherosclerosis models, MSCs and MSC-products result in plaque stabilization and decreased rupture risk.<sup>14,15</sup> Ongoing phase III trials are testing MSC effects on heart function following acute coronary events (i.e. myocardial infarct, MI). Although these trials demonstrated the safety and feasibility of autologous adipose-derived MSCs transplantation in MI donor-related variability, the lack of markers that allow selecting functional MSC leads to inconsistent results (reviewed in Ref.16).

Our group showed that both atherosclerosis and T2DM are independent contributors to the impaired immunopotency (i.e. ability to suppress activated T-cells) of MSCs *in vitro*.<sup>17,18</sup> As MSC immunopotency is a surrogate of their function, the use of autologous MSC in atherosclerosis and T2DM could be associated with suboptimal therapeutic effects. MSCs' pro-inflammatory secretome switch underlies their reduced immunomodulatory effect.<sup>19</sup> The signalling events that trigger a pro-inflammatory secretome in atherosclerosis and T2DM MSC are not fully understood. IKK $\beta$ , via activation of NF- $\kappa$ B, induces the transcription of pro-inflammatory cytokines, chemokines, and inflammatory mediators in adaptive and innate immune cells. However, the role of the IKK $\beta$ -NF- $\kappa$ B pathway in MSC's immunopotency remains elusive. We hypothesized that a constitutive activation of IKK $\beta$  promotes an inflammatory secretome which underlies the impaired immunopotency of MSCs from patients with T2DM and atherosclerosis. We assessed the role of IKK $\beta$  in MSC function and the consequences of its inhibition through pharmacological and gene-editing approaches.

**Table 1** Demographic characteristics of the study subjects

	Control (atherosclerosis) n = 17	T2DM (atherosclerosis +T2DM) n = 17
Gender (F:M)	5:12	5:12
Age (mean ± SD)	57.7±12.3	58.1±12.8
Weight (mean ± SD)	81.2±16.4	87±19.4
Cardiovascular risk factors (%)		
Tobacco	47	18
Hypertension	59	65
Hypercholesterolemia	71	71
Type II diabetes	0	100
Medications (%)		
Aspirin	94	76
Statin	82	70
Metformin	0	82
Insulin	0	27
Glyburide	0	6
Gliclazide	0	6

## 2. Methods

### 2.1 Study subjects

The McGill University Health Center Ethics Review Board (A01-M05-12A) approved the study and participants provided written informed consent. The study conformed to the principles outlined in the Declaration of Helsinki. Subcutaneous adipose tissue was obtained from adults undergoing programmed coronary artery bypass grafting surgery with or without T2DM. Subjects with a history of systemic autoimmune diseases, cancer, and acute or chronic infections were excluded. Table 1 summarizes the demographic characteristics from the donors. In addition, one healthy (Catalog No.: PT-5006) and one T2DM (Catalog No.: PT-5008) human adipose-derived MSCs purchased from Lonza. MSCs were allocated randomly for each experiment.

### 2.2 Isolation, characterization, and stimulation of MSCs

MSCs were isolated from subcutaneous adipose tissue. They were cultured in complete medium (CM) (1.0 g/L glucose, with L-glutamine and sodium pyruvate Dulbecco's modified Eagle's medium (DMEM) (Wisent Biotechnologies, St. Bruno, QC, Canada), supplemented with 10% MSCs qualified foetal bovine serum (FBS) and 1% penicillin/streptomycin (10 000 unit/mL Penicillin, 10 000 mg/mL streptomycin, Life Technologies, Waltham, MA, USA) under standard conditions (5% carbon dioxide; 37°C) in 75-cm<sup>2</sup> tissue culture flasks.

MSCs fulfilled the minimal criteria from the International Society for Cellular Therapy.<sup>20</sup> Immunophenotypic characterization was done by multiparametric flow cytometry (BD LSRII; Becton Dickinson Co, Mountain View, CA). Data were analysed with FlowJo software v9.7.2. For differentiation assays, MSCs were plated at a density of 5000 cells/cm<sup>2</sup> in 24-well plates and incubated with 1 of the 3-differentiation media for 3 weeks as per the manufacturer's protocol (StemPro Adipo-

Osteo-, Chondro-genesis Differentiation Kit). MSCs were then fixed with 4% formaldehyde and stained with Alizarin Red S, Oil red O, or Safranin O to assess osteogenic, adipogenic, and chondrogenic differentiation, respectively. For inflammatory cell signalling studies, MSCs cultured in serum-free medium were pre-treated or not with 30 µM MNL120B (N-(6-chloro-7-methoxy-9H-β-carbolin-8-yl)-2-methylnicotinamide), a highly selective IKKβ inhibitor (a gift from Millennium: The Takeda Oncology Company, Cambridge, MA)<sup>21</sup> and stimulated with 10 ng/mL of TNF-α (10 min) or 5, 10, and 15 µg/mL advanced glycation end products (AGE) products (Sigma Aldrich, Cat No. 121800M).

### 2.3 Flow cytometry analysis for γH2AX

Passage 4 MSCs were fixed in cytofix solution and permeabilized in 0.5% Triton X-100 (Sigma Cat No. 93443) in PBS. After, cells were blocked with 1% BSA, IgG free, protease free, 4% normal donkey serum (Jackson ImmunoResearch, West Grove, PA, USA: Cat No. 001-000-162; Sigma Cat No. D966) and incubated with γH2AX (pS139) antibodies (BD Biosciences, Cat No. 560445). Cells were then washed with PBS and analysed by flow cytometry. Background staining was determined by using same cells. Data were analysed with FlowJo software v9.7.2.

### 2.4 Flow cytometry analysis of ROS

Intracellular ROS was determined using the 2',7'-dichlorodihydrofluorescein diacetate (DCFDA) fluorescent dye. MSCs were stained with DCFDA (10 µM; Sigma) in PBS at 37°C for 30 min. Fluorescence intensity was measured by flow cytometry and background staining was determined by using unstained MSCs. Data were analysed with FlowJo software v9.7.2.

### 2.5 β-Galactosidase staining

β-Galactosidase staining was performed as previously described.<sup>22</sup> Briefly, MSCs were plated 5000 cells/cm<sup>2</sup> in 6-well plates. About 24 h after, cells were washed with PBS and fixed in 0.5% glutaraldehyde solution at RT for 5 min. Following two washes with PBS, cells were incubated with freshly prepared senescence-associated (3-Gal (SA-3-Gal) stain solution at 37°C (without CO<sub>2</sub>). β Galactosidase-positive cells changed the colour into blue within 2–4 h. To detect lysosomal β Galactosidase, the citric acid/sodium phosphate solution was at pH 6.0.

### 2.6 Peripheral blood mononuclear cell isolation, carboxyfluorescein succinimidyl ester (CFSE) fluorescent dye labelling, and peripheral blood mononuclear cell stimulation

Fresh peripheral blood mononuclear cells (PBMCs) from the same donor (36 years old, healthy, female, non-smoker) were used for all experiments. PBMC were isolated via Ficoll gradient centrifugation and cultured overnight in 10% FBS RPMI (Wisent Biotechnologies) medium to deplete monocytes. Immunopotency assay: The capacity of MSCs to suppress proliferation of activated CD4<sup>+</sup> T-cells was assessed in a co-culture system. MSCs were plated at 75 × 10<sup>3</sup> cells per well in flat-bottom 24-well plates (Corning, Corning, NY, USA) and cultured overnight at 37°C, 5% CO<sub>2</sub>. The next day, monocyte-depleted PBMCs were stained with 10 µM CFSE (Sigma) and stimulated with anti-CD3/CD28 beads (1 bead per cell) (Dynabeads Human T-Activator CD3/CD28, Life Technologies). CFSE-stained PBMCs (6 × 10<sup>5</sup>) were cultured for 4 days with MSCs either in cell-cell contact-dependent (direct co-cultures) or in contact-independent conditions (trans-well cultures) (MSCs: PBMCs

ratio 1:8). In the trans-well system, MSCs and T-cells were separated by a 0.4  $\mu$ m pore size membrane (Millipore, Etobicoke, ON, Canada). At Day 4, Flow cytometry analysis (BD FACS Canto II flow cytometer equipped with BD FACSDiva Software v8.0.1) was done. To evaluate the functional implications of inhibiting interleukin (IL)-6 on MSCs' immunopotency, neutralization assays were performed by adding either anti-IL-6 antibody (20  $\mu$ g/ml) (R&D Systems, Cat No. MAB206) or isotope control (20  $\mu$ g/ml) (R&D Systems, Cat No. MAB002) at the beginning of the co-cultures.

## 2.7 PBMC migration assays

MSCs (50 000) were seeded in 24-well plates with 0.5 mL CM. After 24 h, conditioned medium was collected and transferred into the lower chamber of trans-wells (24-well 8- $\mu$ m, Costar). PBMCs ( $1 \times 10^6$  in 300  $\mu$ L) were loaded to the upper chamber. Plates were incubated for 3 h under standard conditions and transmigrated cells were counted.

## 2.8 Lentiviruses production and transduction

Six different human IKK $\beta$  guide RNAs (gRNAs) (see [Supplementary material online, Table S1](#)) and non-targeting gRNAs were purchased from GenScript (NJ, USA) and sub-cloned in pLentiCRISPR v2 using BsmBI restriction site (Addgene Plasmid No. 52961). VSV-g-pseudotyped lentiCRISPR virions were produced in HEK293FT cells using lipofectamine 3000 (Cat No. L3000015) with 1.5  $\mu$ g pMDLg/pRRE, 1.5  $\mu$ g pRSV-REV, and 3  $\mu$ g pVSV-G with 6  $\mu$ g of pLentiCRISPR v2 vectors. Viral supernatants were harvested after 72 h and used to transduce primary MSCs by infection in the presence of 10  $\mu$ g mL<sup>-1</sup> polybrene. Transduced cells were selected with 1.5  $\mu$ g mL<sup>-1</sup> puromycin at Day 3 post-transduction and used within 7 days.

## 2.9 Enzyme-linked immunosorbent assays

MSCs were plated in 6-well plates at a density of  $1 \times 10^5$  cells/well in 2 mL CM. To establish difference between atherosclerosis+ T2DM, atherosclerosis MSCs, they were cultured for 4 days and supernatants were collected for enzyme-linked immunosorbent assays (ELISA from Life Technologies) according to the manufacturer's instructions (i.e. IL-6, IL-8/C-X-C motif chemokine ligand 8 (CXCL8), monocyte chemoattractant protein (MCP-1/CCL2). For selective IKK $\beta$  inhibitor (i.e. MLN120B) treatment experiments, MSCs were plated in 6-well plates at a density of  $1 \times 10^5$  cells/well. After 24-h treatments with either 30  $\mu$ M MLN120B or vehicle (DMSO 0.1%), cells were washed with PBS and CM was added. After 24 h, the supernatants were collected and tested by ELISA.

To quantify T-loop phosphorylation of IKK $\beta$  at Ser177/181, MSCs were plated in 6-well plates at a density of  $1 \times 10^5$  cells/well. About 48 h after cells were harvested according to the manufacturer's instructions for PathScan<sup>®</sup> Phospho-IKK $\beta$  (Ser177/181) Sandwich ELISA Kit No. 7080 (Cell Signaling Technology, Danvers, MA).

## 2.10 Western blotting

MSCs were cultured with CM for 72 h and whole cell extracts (WCE) were prepared using RIPA lysis buffer complemented with protease inhibitors (50 mM Tris, pH 7.4; 150 mM NaCl; 50 mM NaF; 5 mM EDTA; 10% glycerol; 1 mM Na<sub>3</sub>VO<sub>4</sub>; 40 mM  $\beta$ -glycerophosphate; 0.1 mM phenylmethylsulphonyl fluoride; 5  $\mu$ g/mL of leupeptin, pepstatin, and aprotinin; 1% Triton X-100; 1% Sodium deoxycholate; 0.1% sodium dodecyl sulphate) for 30 min on ice. Lysates were clarified by centrifugation at 13 000 g for 10 min, and equal amounts of protein (30–60  $\mu$ g) were

subjected to electrophoresis on 7.5–12% acrylamide gels. Proteins were electrophoretically transferred to Hybond-C nitrocellulose membranes (Amersham) in 25 mM Tris and 192 mM glycine. In some western-blot experiments, cellular extracts were equally divided ( $\mu$ g) and used in parallel on the same or different SDS-polyacrylamide gels. SDS gels containing electrophoresed proteins were simultaneously electrotransferred onto nitrocellulose membranes.

Immunoblot analysis for each antibody listed in [Supplementary material online, Table S2](#), was carried out according to manufacturer's instructions. Signals were detected with a chemiluminescence system (ECL Plus, Amersham).

## 2.11 Myocardial infarction model

All animal experiments have ethics approval from the animal care committee of Université de Montréal (No. 14-035) and all animal procedures conform to the NIH guidelines (No. A5213-01). An acute MI (AMI) was created in 8-month-old male C57BL/6 mice (Jackson Laboratory) by permanent ligation of the left anterior descending (LAD) artery (permanent LAD occlusion model).<sup>23</sup> Briefly, mice were anaesthetized with 3% isoflurane mixed with 100% oxygen, intubated (20 G catheter Cathlon<sup>®</sup>), and ventilated with a tidal volume of 220  $\mu$ L at a rate of 130 strokes/min (settings for a mouse weighing 30 g, and readjusted according to weight), with a MiniVent type rodent ventilator (Harvard Apparatus). Anaesthesia was kept with 2% isoflurane and the temperature of the animals was maintained with a heating pad. Mice received an injection of lidocaine (6 mg/kg) in the intercostal muscles prior to a left lateral incision (third intercostal space) to provide heart exposure. The LAD was ligated with a 8-0 nylon thread under a Nikon SMZ645 stereomicroscope with a magnification of 0.8 $\times$  to 5 $\times$ . Immediately after AMI induction, the region at risk is visualized by its paleness and the mice was randomized to receive one of the following treatments: saline, atherosclerosis MSCs, atherosclerosis+T2DM-MSCs, atherosclerosis+T2DM Scramble MSCs (gRNA-negative control), or atherosclerosis+T2DM IKK $\beta$  knockdown (KD) MSCs (encoding gRNA molecule no. 2). MSCs were injected intramyocardially around the area at risk in five injections of 5  $\mu$ L each (20 000 cells). Mice received a s.c. injection of buprenorphine SR (1 mg/kg) prior to recovery. About three animals in atherosclerosis MSC-injected group died within the 30 min of the injection. After 4 days, animals were sacrificed by exsanguination under isoflurane anaesthesia and processed. Hearts were collected following 10 mL of ice-cold saline perfusion into the left ventricular apex. Hearts were fixed for 24 h in Formalin and paraffin embedded at the Institute for Research in Immunology and Cancer (IRIC) Histology core facility (Université de Montréal). Paraffin blocks were cut into 4  $\mu$ m sections. Haematoxylin and eosin stain were done for general morphology and immunohistochemistry to demonstrate monocytes/macrophages (MOMA-2), CD4, and FOXP3 infiltration with the automated Bond RX staining platform from Leica Biosystems, Australia). Sections were deparaffinized inside the immunostainer. Antigen recovery was conducted using Proteolytic-Induced Epitope Retrieval with Enzyme 1 (Leica Biosystems proprietary reagent). Sections were then incubated with 150  $\mu$ L of anti-MOMA2, anti CD4, and anti-FOXP3 antibody. Detection of specific signal was acquired by using Bond Polymer DAB Refine kit (No. DS9800, Leica Biosystems) with a rabbit anti-rat antibody (Vector Laboratories, 1/200). Stained slides were coverslipped and scanned using the Hamamatsu's NanoZoomer<sup>®</sup> Digital Pathology system 2HT and visualized with NDP.view2.

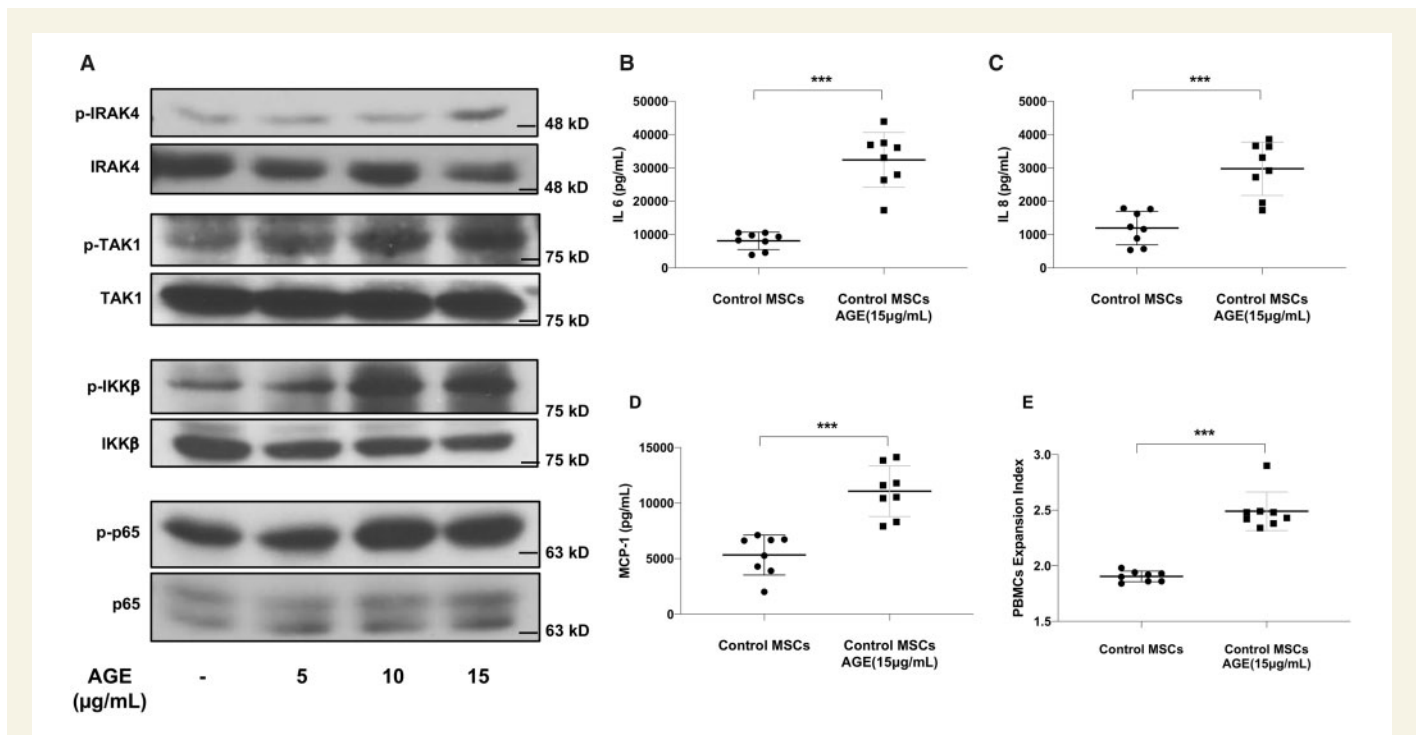


**Figure 1** Advanced glycolytic end (AGE) products activates IKK $\beta$  signalling cascade and reduce Mesenchymal stromal cells (MSCs) immunopotency. (A) Western-blot analysis representative of two independent experiments with similar results showing the activation of the IRAK4–TAK1–IKK $\beta$ –p65/NF- $\kappa$ B signalling cascade on healthy MSCs that are exposed to 5, 10, and 15  $\mu$ g/mL AGE products for 24 h. (B–D) AGE induced an increase in the production of IKK $\beta$ –NF- $\kappa$ B-regulated pro-inflammatory cytokine IL-6 (\*\* $^*P$  = 0.0002,  $n$  = 8), and chemokines IL-8/CXCL8 (\*\* $^*P$  = 0.0006,  $n$  = 8), MCP-1/CCL2 (\*\* $^*P$  = 0.0002,  $n$  = 8). (E) Reduced immunosuppressive function of MSCs after AGE products (\*\* $^*P$  = 0.0002,  $n$  = 8). Each dot represents different biological replicates (i.e. single healthy control MSCs). Mann–Whitney  $U$  test was used to compare two independent groups. Abbreviations: MSCs, mesenchymal stromal cells; TAK-1, transforming growth factor- $\beta$ -activating kinase1; IKK $\beta$ , inhibitor of nuclear kappa-B kinase subunit beta; p65, nuclear factor kappa-light-chain-enhancer of activated B cells RelA subunit; IRAK4, interleukin-1 receptor-associated kinase 4; IL-6, interleukin-6; IL-8, interleukin-8; MCP-1, monocyte chemoattractant protein-1; PBMCs, peripheral blood mononuclear cells.

## 2.12 Statistical analysis

Analyses were performed with GraphPad Prism software v8 (GraphPad, San Diego). Graphs are presented as dot plots. Mann–Whitney  $U$  test was used to compare differences between two independent groups (atherosclerosis and atherosclerosis+T2DM MSCs). Wilcoxon test was used to compare paired groups (atherosclerosis +T2DM MSCs  $\pm$  MLN120B or IKK  $\beta$  KD). All hypotheses tests were 2-sided; a  $P$  < 0.05 was considered significant and is indicated by an asterisk in the figures.

## 3. Results

### 3.1 AGE products reduce MSCs immunopotency

AGE products are known to contribute development atherosclerosis in T2DM patient. They have the ability to disrupt cell structure and lead to cellular dysfunction. Moreover, AGE products have been shown to contribute both the micro- and macrovascular complications of T2DM.<sup>24</sup> To determine whether AGE products alters MSC immunopotency, we first treated MSCs with different doses (5, 10, and 15  $\mu$ g/mL) of AGE product (Figure 1A). AGE treatment activated the canonical IRAK4–TAK1–IKK $\beta$  inflammatory signalling cascade<sup>25</sup> culminating in increased phosphorylation of the transactivation domain of the p65 NF- $\kappa$ B subunit (Ser536), a process

involved in its transcriptional activity<sup>26</sup> (Figure 1A). We next assessed AGE-treated MSCs' IKK $\beta$ –NF- $\kappa$ B associated pro-inflammatory cytokine including IL-6 (Figure 1B), chemokines IL-8/CXCL8 (Figure 1C), and MCP-1/CCL2 (Figure 1D). Importantly, treatment with the AGE product also reduced efficiency to suppress PBMCs proliferation (Figure 1E).

### 3.2 MSCs from T2DM patients with atherosclerosis have senescence features

Given that T2DM and atherosclerosis are age-related diseases, we assessed whether adipose-derived MSCs from atherosclerotic T2DM patients displayed hallmarks of chronic cellular senescence. We compared the phenotype of atherosclerosis+T2DM MSCs ( $n$  = 17) to those of age- and sex-matched atherosclerotic non-T2DM (atherosclerosis MSCs) ( $n$  = 17). MSCs samples were randomly distributed for all the experiments. Markers of cellular senescence, including enlarged cell size (see Supplementary material online, Figure S1A), increased intracellular ROS levels (see Supplementary material online, Figure S1B),  $\gamma$ H2AX content (see Supplementary material online, Figure S1C), autofluorescence<sup>27</sup> (see Supplementary material online, Figure S1D), and the proportion of X-GAL-positive cells (see Supplementary material online, Figure S1E) were higher in atherosclerosis+T2DM MSCs. In addition, atherosclerosis+T2DM MSCs displayed reduced proliferation ability (see Supplementary material online, Figure S1F) compared to atherosclerosis MSCs. Moreover, atherosclerosis+T2DM MSCs showed an

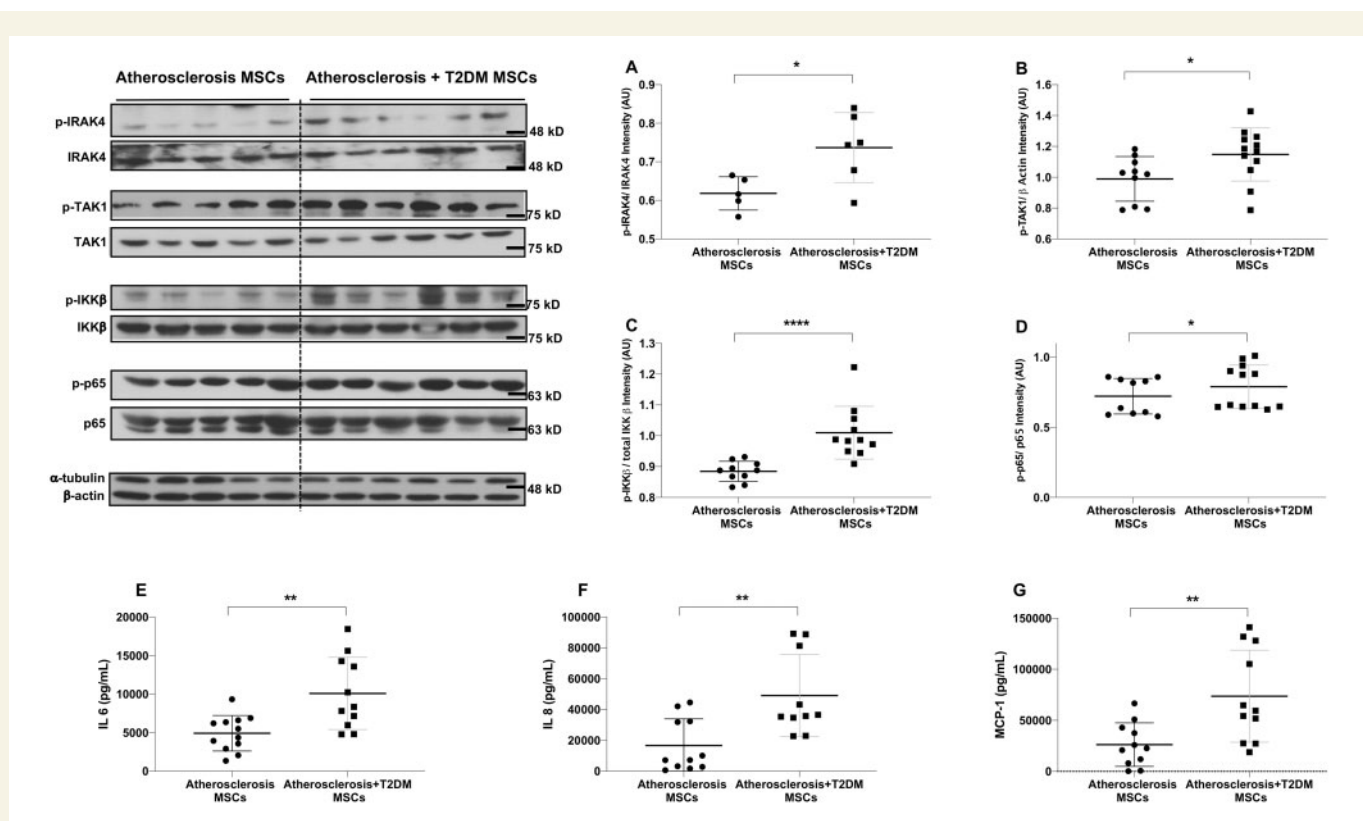


**Figure 2** Constitutively activated forms of inflammation-activated protein kinases and increased pro-inflammatory cytokine secretion in atherosclerosis+T2DM MSCs. Augmented active T-loop phosphorylated forms of (A) IRAK 4 (\* $P = 0.05$ , atherosclerosis MSCs  $n = 5$ , atherosclerosis+T2DM MSCs  $n = 6$ ), (B) TAK1 (\* $P = 0.02$ , atherosclerosis MSCs  $n = 10$ , atherosclerosis+T2DM MSCs  $n = 12$ ) and (C) IKK $\beta$  (\*\*\*\* $P < 0.000$ , atherosclerosis MSCs  $n = 10$ , atherosclerosis+T2DM MSCs  $n = 11$ ); (D) Increased phosphorylation of p65 NF- $\kappa$ B transcription factor on Ser536 located in its transactivation domain (\* $P = 0.05$ , atherosclerosis MSCs  $n = 10$ , atherosclerosis+T2DM MSCs  $n = 12$ ) and (E–G) Increased production of IKK $\beta$ –NF- $\kappa$ B-dependent pro-inflammatory cytokine IL-6 (\*\*\* $P = 0.0002$ , atherosclerosis MSCs  $n = 12$ , atherosclerosis+T2DM MSCs  $n = 11$ ), and chemokines IL-8/CXCL8 (\*\*\* $P = 0.0006$ , atherosclerosis MSCs  $n = 11$ , atherosclerosis+T2DM MSCs  $n = 10$ ), MCP-1/CCL2 (\*\*\* $P = 0.0002$ , atherosclerosis MSCs  $n = 11$ , atherosclerosis+T2DM MSCs  $n = 11$ ). Each dot represents different biological samples (i.e. MSC from different donors). Mann–Whitney  $U$  test was used to compare two independent groups. Abbreviations: T2DM, type 2 diabetes mellitus; MSCs, mesenchymal stromal cells; TAK-1, transforming growth factor- $\beta$ -activating kinase1; IKK $\beta$ , inhibitor of nuclear factor kappa-B kinase subunit beta; p65, nuclear factor kappa-light-chain-enhancer of activated B cells RelA subunit; IRAK4, interleukin-1 receptor-associated kinase 4; IL-6, interleukin-6; IL-8, interleukin-8; MCP-1, monocyte chemoattractant protein-1.

increase in the expression levels for IL1 $\beta$ , p-p53 (Ser15), and anti-apoptotic markers B-cell lymphoma (Bcl)-2 and Bcl-XL proteins (see [Supplementary material online, Figure S1G](#)).

### 3.3 MSCs from T2DM patients with atherosclerosis have constitutive activation of IKK $\beta$

The observed DNA damage, high intracellular ROS levels, decrease proliferation, and the presence of an increase expression of anti-apoptotic effectors under the control of NF- $\kappa$ B<sup>28</sup> likely indicate the activation of pro-inflammatory signalling cascades in senescent atherosclerosis+T2DM MSCs and probably reflects what is observed in AGE-exposed MSCs (Figure 1). Considering that IKK $\beta$  is a master regulator of inflammatory response signalling events and presumably engaged in this deregulated response, we next tested whether atherosclerosis+T2DM MSCs have an ‘IKK $\beta$  signature’: activated (i.e. T-loop phosphorylated) forms of IKK $\beta$  and their upstream and downstream signalling effectors. Atherosclerosis+T2DM MSCs constitutively expressed higher

levels of phosphorylated forms of IRAK4 (Figure 2A), the IKK $\beta$ -activating kinase transforming growth factor- $\beta$ -activating kinase1 (TAK-1)<sup>29</sup> (Figure 2B) and IKK $\beta$  (Figure 2C and see [Supplementary material online, Figure S2](#)), culminating in increased phosphorylation of the p65 NF- $\kappa$ B subunit (Figure 2D). Importantly, this constitutive ‘IKK $\beta$  signature’ correlated with the production of pro-inflammatory components including IL-6 (Figure 2E), IL-8/CXCL8 (Figure 2F), and MCP-1/CCL2 (Figure 2G).

### 3.4 Atherosclerosis+T2DM MSCs display impaired immunopotency both *in vitro* and *in vivo*

We next evaluated whether the constitutive IKK $\beta$  signature observed in senescent atherosclerosis+T2DM MSCs affected their immunomodulatory properties. Using cell–cell contact conditions, the proliferation of CD4<sup>+</sup> T-cell –a read-out that inversely correlates with MSC immunomodulatory function was higher in atherosclerosis+T2DM MSCs than in atherosclerosis MSCs (Figure 3A), an effect that was not explained by differential MSCs-induced T-cell apoptosis (Figures 3B). To assess the

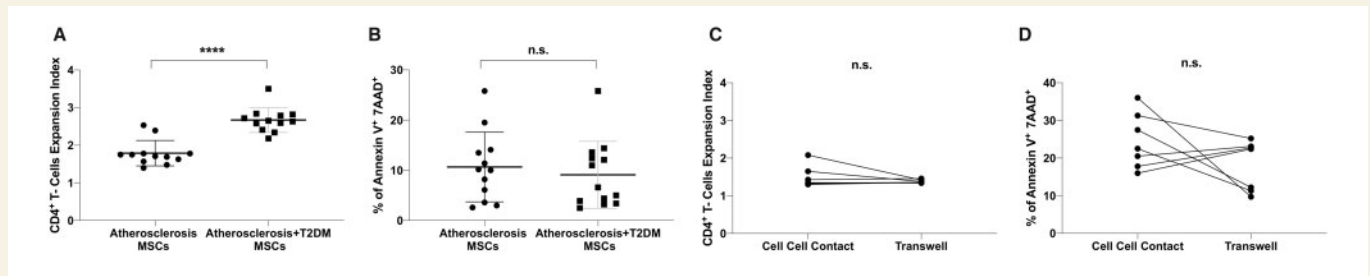


**Figure 3** Impaired immunosuppressive abilities of atherosclerosis+T2DM MSCs *in vitro*. (A–D) MSCs immunomodulatory capacity was assessed in T cell co-cultured in cell–cell contact-dependent and -independent (trans-well) conditions. (A) In cell–cell contact condition, a decreased immunopotency in atherosclerosis+T2DM MSCs compared to atherosclerosis MSCs (\*\*\*\* $P = 0.0001$ , atherosclerosis MSCs  $n = 12$ , atherosclerosis+T2DM MSCs  $n = 12$ ). This is independent of the viability of activated CD4<sup>+</sup> T cells (atherosclerosis MSCs  $n = 12$ , atherosclerosis+T2DM MSCs  $n = 13$ ) (B). (C) Similar immunopotency in both cell–cell contact and trans-well conditions ( $n = 7$ ) and (D) CD4<sup>+</sup> T cell viability in trans-well conditions ( $n = 7$ ). Each dot represents different biological samples (i.e. MSC from different donors). Mann–Whitney  $U$  test was used to compare two independent groups and Wilcoxon test was used for paired comparisons. Abbreviations: T2DM, type 2 diabetes mellitus; MSCs, mesenchymal stromal cells; 7-AAD, 7-aminoactinomycin D.

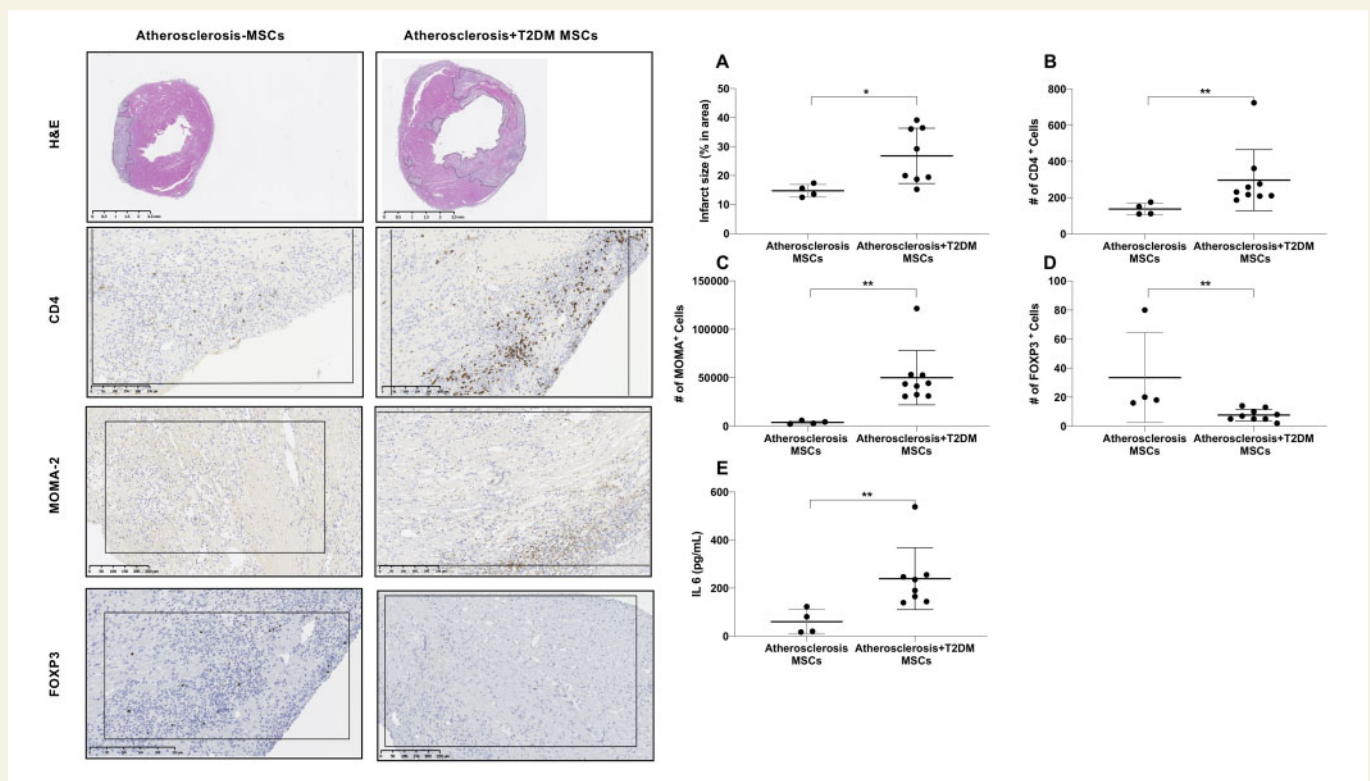
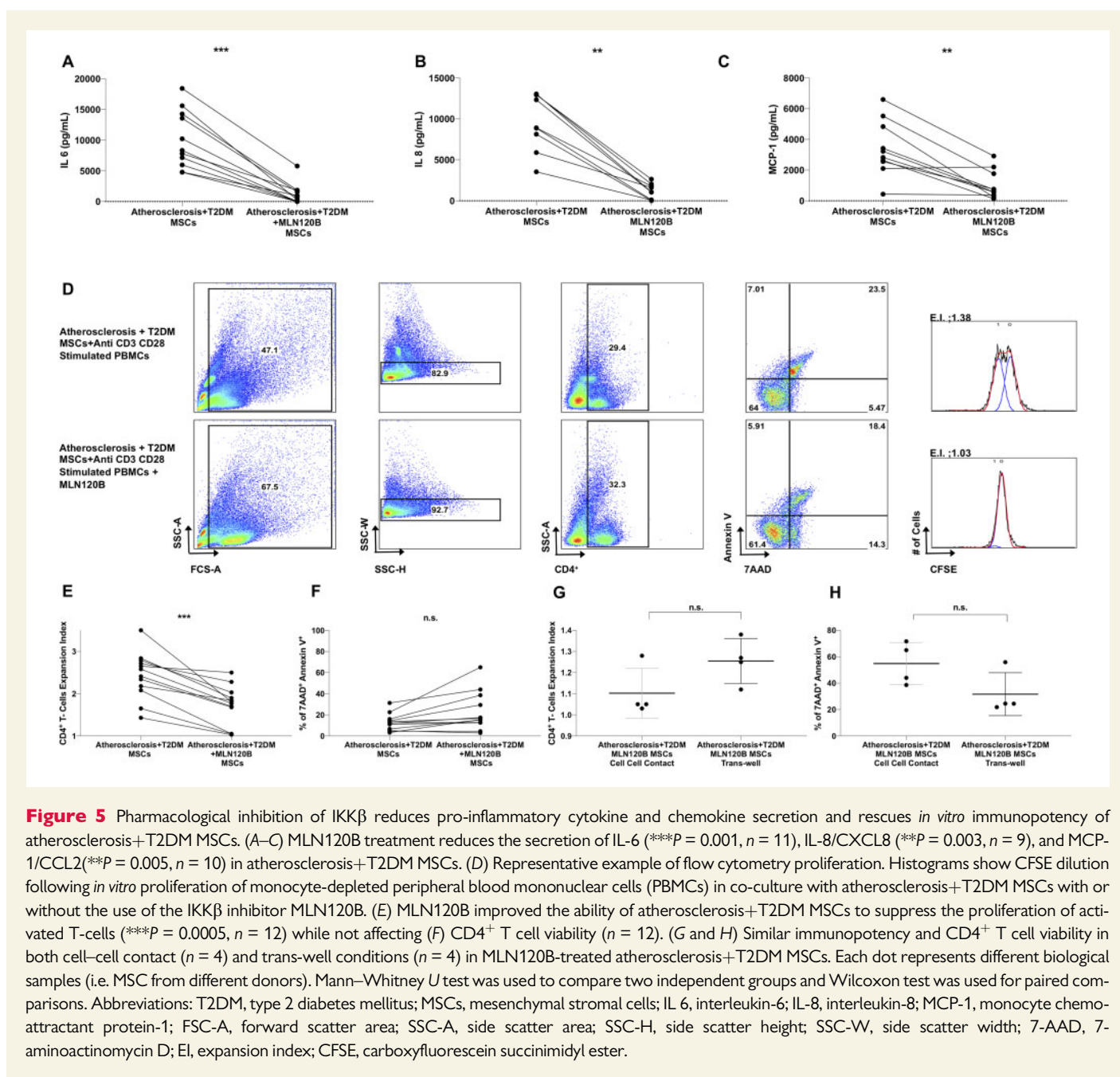


**Figure 4** Atherosclerosis+T2DM-MSCs have reduced immunopotency *in vivo*. (A) Haematoxylin and Eosin (H&E) staining of the injured (i.e. purple: infiltration of leucocytes) and viable myocardium (i.e. pink) (\* $P = 0.01$ , atherosclerosis MSCs  $n = 4$ , atherosclerosis+T2DM MSCs  $n = 8$ ), (B) CD4<sup>+</sup> (\*\* $P = 0.002$ , atherosclerosis MSCs  $n = 4$ , atherosclerosis+T2DM MSCs  $n = 9$ ), (C) Monocyte/macrophage (MOMA-2 staining) (\*\* $P = 0.002$ , atherosclerosis MSCs  $n = 4$ , atherosclerosis+T2DM MSCs  $n = 9$ ), and (D) FOXP3 (\*\* $P = 0.002$ , atherosclerosis MSCs  $n = 4$ , atherosclerosis+T2DM MSCs  $n = 9$ ) content in heart sections and (E) IL-6 plasma levels (\* $P = 0.02$ , atherosclerosis MSCs  $n = 4$ , atherosclerosis+T2DM MSCs  $n = 8$ ). Each dot represents different animals injected with different biological samples (i.e. MSC from different donors). Mann–Whitney  $U$  test was used to compare two independent groups. Abbreviations: T2DM, type 2 diabetes mellitus; MOMA, monoclonal anti-macrophage antibody; IL 6, interleukin-6.

relevance of soluble factors as mediators of MSCs: T-cell suppression, we next conducted cell–cell contact-dependent and -independent (trans-well) co-cultures. Our results showed similar T-cell suppression capacity (Figure 3C) and CD4<sup>+</sup> T cells apoptosis rate (Figure 3D) in both

trans-well and cell–cell contact conditions. However, MSC survival in atherosclerosis+T2DM MSCs after co-culturing with PBMCs was lower compared to atherosclerosis MSCs (see [Supplementary material online, Figure S3A and B](#)). These results indicated that MSCs' ability to suppress T-cell



proliferation is mediated by secreted factors. Moreover, atherosclerosis +T2DM MSCs not only displayed reduce immunopotency but they were more prone to undergo apoptosis upon co-culture with PBMCs.

To evaluate whether *in vitro* findings translate *in vivo*, we used the permanent left anterior descending (LAD) occlusion model for acute MI atherosclerosis and atherosclerosis+T2DM MSCs was injected intra-myocardially before the ligation. Animals were sacrificed 4 days after injection where the survival rates of the injected MSCs were similar in both groups (see [Supplementary material online, Figure S4](#)). Immunohistochemical analysis of heart sections showed an increased infarct size ([Figure 4A](#)), CD4 $^{+}$  T cell ([Figure 4B](#)), monocyte/macrophage infiltration ([Figure 4C](#)), and decreased FOXP3 ([Figure 4D](#)) content in the heart sections, correlating with increased levels of circulating IL-6 in atherosclerosis+T2DM MSCs injected animals.

### 3.5 IKK $\beta$ inhibition in atherosclerosis+T2DM MSCs improves their immunopotency *in vitro*

Pharmacological pre-conditioning of MSCs, prior to transplantation improves their therapeutic effects via changes in their secretome.<sup>30,31</sup> Given the role of IKK $\beta$  in regulating inflammatory gene transcription and mRNA translation,<sup>32</sup> and the presence of an IKK $\beta$  signature in senescent atherosclerosis+T2DM MSCs, we next evaluated the effects of inhibiting IKK $\beta$  on MSCs' immunopotency. Pre-treatment of atherosclerosis+T2DM MSCs with MLN120B, a potent pharmacological IKK $\beta$  inhibitor<sup>21</sup> (see [Supplementary material online, Figure S5](#)), reduced the production of IL-6 ([Figure 5A](#)), IL-8/CXCL8 ([Figure 5B](#)) and MCP-1/CCL2 ([Figure 5C](#)) and enhanced their



immunopotency (Figure 5D and E) without modifying T-cell apoptosis (Figure 5F). These results were similar in both trans-well and cell–cell contact conditions (Figure 5G and H). Interestingly pre-treatment of MLN120B in atherosclerosis MSCs did not have an impact on their IL-6 and MCP-1/CCL2 production (see [Supplementary material online, Figure S6](#)).

We previously reported that compared to healthy controls, atherosclerosis-MSCs have impaired immunomodulatory function mediated by a pro-inflammatory secretome.<sup>17</sup> We also showed that neutralizing inflammatory-secreted factors partially restores the immunopotency of atherosclerosis-MSCs *in vitro*.<sup>17,19</sup> Among the SASP components, IL-6 is a pivotal signalling cytokine in the innate immune cascade thought to mediate MSC's immunopotency. Moreover, IL-6 secretion is suggested as a marker for senescence.<sup>33</sup> Thus, we focused on IL-6 secretion levels as a surrogate marker for SASP. Exogenously added IL-6 impaired the immunosuppressive ability of cultured atherosclerosis MSCs (dose-dependent effect, see [Supplementary material online, Figure S7A](#)). Moreover, we observed a positive correlation between the production of IL-6 by cultured MSCs and the proliferation of activated T cells, reflecting a decrease in MSCs' immunopotency (see [Supplementary material online, Figure S7B and C](#)).

### 3.6 IKK $\beta$ inhibition rescues the therapeutic efficacy of atherosclerosis+T2DM MSCs *in vivo*

Although MLN120B improves atherosclerosis+T2DM MSCs immunopotency *in vitro*, this effect is limited to 24 h (see [Supplementary material online, Figure S5](#)). To increase the duration of the anti-inflammatory targeted approach, we next employed a genetic loss-of-function approach using clustered regularly interspaced short palindromic repeats (CRISPR)/Cas9 gene-editing tool targeting *IKBKB* to silence the *IKK $\beta$*  signature of atherosclerosis+T2DM MSCs. MSCs were retrovirally transduced with the two most efficient gRNA molecules (out of 6; see [Supplementary material online, Figure S8](#)) to generate populations of cells where the activated forms of both IKK $\beta$  and p65 compared to scramble non-targeting gRNA sequence controls (Figure 6A). Importantly, CRISPR-mediated *IKBKB* gene disruption not only enhanced the immunomodulatory capacity of atherosclerosis+T2DM MSCs (Figure 6B) by significantly reducing their pro-inflammatory secretome (see [Supplementary material online, Figure S9](#)) and their survival capacity (see [Supplementary material online, Figure S10](#)) but also prevented the chemoattraction of immune system cells that is seen in atherosclerosis+T2DM MSCs (Figure 6C).

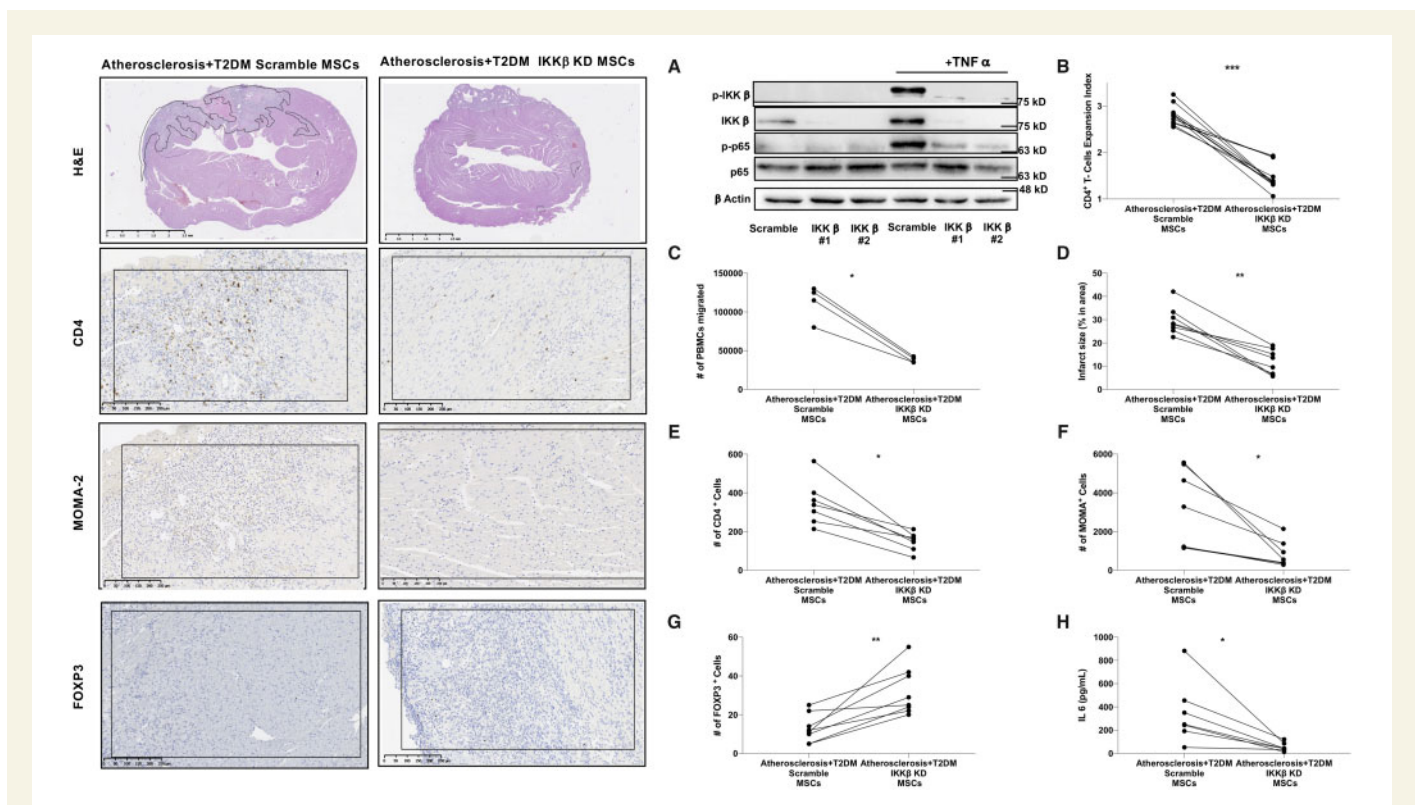


**Figure 6** IKK $\beta$  knockdown in atherosclerosis+T2DM-MSCs enhances their immunoprotective effects in the permanent LAD ligation model. (A) Representative western blots showing the efficacy of two different gRNA molecules targeting the *IKBKB* locus in one control MSCs left either untreated or exposed to 10 ng/mL TNF- $\alpha$  for 10 min. Note that the KD efficiency was evaluated in all the MSCs samples used *in vivo* (see [Supplementary material online, Figure S11](#)). The effect of reducing the expression level of IKK $\beta$  in atherosclerosis+T2DM MSCs was evaluated on their (B) immunopotency *in vitro* (\*\* $P = 0.001$ ,  $n = 11$ ) and (C) ability to attract PBMCs (\* $P = 0.02$ ,  $n = 4$ ). (D) Haematoxylin and Eosin (H&E) staining of the injured (i.e. purple: infiltration of leucocytes) and viable myocardium (i.e. pink) (\*\* $P = 0.007$ ,  $n = 8$ ), (E) CD4 $^+$  (\* $P = 0.01$ ,  $n = 7$ ), (F) Monocyte/macrophage (MOMA-2 staining) (\* $P = 0.01$ ,  $n = 7$ ), and (G) FOXP3 (\*\* $P = 0.007$ ,  $n = 8$ ) content in heart sections and (H) IL-6 plasma levels (\* $P = 0.01$ ,  $n = 7$ ) were assessed. Each dot represents different animals injected with six different biological samples (i.e. MSC from different donors). Wilcoxon test used for paired groups. Abbreviations: T2DM, type 2 diabetes mellitus; PBMCs, peripheral blood mononuclear cells; MOMA, monoclonal anti-macrophage antibody; IL 6, interleukin-6.

After rescuing *in vitro* immunopotency of atherosclerosis+T2DM MSCs by targeting IKK $\beta$ -NF- $\kappa$ B axis, we next investigated whether similar approach would rescue their *in vivo* healing capacity. The intra-myocardial injection of atherosclerosis+T2DM IKK $\beta$  KD MSCs (see [Supplementary material online, Figure S11](#)) following LAD ligation reduced the infarcted area compared to that in animals treated with atherosclerosis+T2DM Scramble MSCs or saline ([Figure 6D](#) and see [Supplementary material online, Figure S12](#)). Immunohistochemical analysis of heart sections confirmed a decrease in CD4<sup>+</sup> T cell ([Figure 6E](#)), monocyte/macrophage ([Figure 6F](#)) and increase in FOXP3 ([Figure 6G](#)) content in the heart sections. Further, plasma IL-6 levels, which in MI correlate with the infarct size and a reduced left ventricular ejection fraction,<sup>34</sup> were lower in the atherosclerosis+T2DM IKK $\beta$  KD MSCs ([Figure 6H](#)).

## 4. Discussion

The success of MSC-based therapies in pre-clinical models of MI has not been consistently confirmed in clinical trials.<sup>35</sup> In part this relates to the fact that MSCs function is donor-dependent. Donor's age and inflammatory status have detrimental effects on MSCs function which can affect therapeutic outcomes.<sup>36</sup> Previously, we showed that age and age-related conditions such as atherosclerosis and T2DM alter MSCs immunomodulatory function (i.e. MSC-mediated inhibition of CD4<sup>+</sup> T cell proliferation in allogeneic co-cultures).<sup>18</sup> Within the aforementioned groups atherosclerosis+T2DM MSCs displayed the most severe impairment in immunomodulatory function. Here, we demonstrate that atherosclerosis+T2DM MSCs display two features of cellular senescence: a SASP and an IKK $\beta$  molecular signature. High levels of constitutively active IKK $\beta$  switches the secretome of atherosclerosis+T2DM MSCs towards pro-inflammatory and impairs their ability to suppress CD4<sup>+</sup> T-cell proliferation. We also show that genome editing of atherosclerosis+T2DM MSCs selectively inhibiting the constitutively activated form of IKK $\beta$  enhances their immunosuppressive functions.

Our data suggest that AGE product exposure in atherosclerosis+T2DM MSCs are major contributors to the chronic activation of the IKK $\beta$ -NF- $\kappa$ B pathway and a SASP.<sup>37,38</sup> AGE products and their receptors (receptors for advanced glycation end products: RAGEs) are highly expressed in unstable angina and accelerated atherosclerosis in subjects with T2DM.<sup>1</sup> Moreover, targeting RAGE in animal models of diabetes with accelerated atherosclerosis ameliorates atherosclerotic plaque development by reducing vascular oxidative stress and inflammation.<sup>39</sup> RAGEs are also implicated in myocardial dysfunction and mitochondrial-oxidative stress in high-fat-fed mice.<sup>40</sup> In addition to increase the levels of ROS and induce mitochondrial dysfunction, AGEs also activate key cell signalling pathways including the IKK $\beta$ /NF- $\kappa$ B pathway, which modulate the expression of proinflammatory genes.<sup>41</sup> Our data indicate the detrimental effects of AGE products in MSCs' functions. AGE exposure activates the IKK $\beta$ /NF- $\kappa$ B pathway which then increase the production of proinflammatory secretome and reduce MSCs' immunopotency. Although RAGE modulation through antagonist peptides has been described<sup>42-44</sup> due to complexity of RAGE signalling pathway and its important roles in both tissue injury and in resolving the pathogenesis, it is considered as double-edged sword. Moreover, as seen in our study pharmacological inhibitors' (i.e. MLN120B) *ex vivo* potency to rescue the immunomodulatory functions of atherosclerosis+T2DM MSCs is transient and not as potent as the stable *ex vivo* depletion of IKK $\beta$ .

Increasing circulating levels of IL-6 and its receptor (IL-6R), are associated with increased risk of cardiovascular events and poor outcomes post-acute MI.<sup>45,46</sup> High levels of IL-6 at the time of MI are associated

with greater myocardial injury and reduced myocardial reperfusion following percutaneous coronary interventions.<sup>46,47</sup> In a large case-control study, circulating IL-6R levels were associated with higher risk of all causes and cardiovascular mortality in individuals with ST-elevation MI.<sup>45</sup> Here, we showed that MSCs from T2DM+atherosclerosis individuals secrete higher levels of IL-6. Given the wide tissue distribution of MSCs, the constitutive pro-inflammatory secretome of atherosclerosis+T2DM MSCs could promote *in vivo* inflammatory auto-feedback mechanisms (i.e. through the reduced immunopotency) enhancing the atherosclerotic risk of T2DM. The intra-myocardial administration of atherosclerosis +T2DM MSCs to an AMI mice model resulted in greater infarct size and higher plasma levels of IL-6. The high IL-6 plasma levels are indicators of higher degree of myocardial injury and increased lymphocytic infiltration and may predict an increased risk of heart failure. The demonstration of MSC immunopotency is a prerequisite for advanced MSCs clinical trials (reviewed in Ref.48). The quality of MSCs prior to transplantation determines post-transplant effects. Targeting IKK $\beta$  via gene editing reduced the secretion of pro-inflammatory cytokines by atherosclerotic+T2DM MSCs, but also the extension of MI and IL-6 plasma levels in the LAD-MI model. It is worth mentioning that the survival of atherosclerotic+T2DM MSCs was also enhanced following the inhibition of IKK $\beta$ .

To our knowledge, this study is the first to demonstrate that *ex vivo* gene editing modifies the impaired immunomodulatory function of MSCs from individuals with atherosclerosis and T2DM. Additional studies are required to establish the relevance of the IKK $\beta$ -NF- $\kappa$ B axis in MSCs in the clinical setting. In summary, this study shows that MSCs from individuals with atherosclerosis and T2DM have a senescent phenotype and constitutive activation of IKK $\beta$ . They have a pro-inflammatory secretome that mediates their impaired immunopotency. Gene editing of IKK $\beta$  reduced T2DM MSCs's proinflammatory secretome and i) enhanced their immunomodulatory function; ii) reduced their chemoattractive ability; and iii) increased their survival rate. Overall our data suggest that the efficacy of atherosclerosis + T2DM MSCs in clinical settings could be compromised compared to those of non-T2DM subjects. In addition, we demonstrated that IKK $\beta$  is a candidate to enhance the function of T2DM-MSC for their use in the autologous setting.

## Supplementary material

Supplementary material is available at *Cardiovascular Research* online.

**Conflict of interest:** none declared.

## Funding

This work was supported by research grants from the Canadian Institutes of Health Research (CIHR; MOP-123482) and the Heart and Stroke Foundation of Canada (HSFC; G-16-00014208) to M.J.S. M.J.S. holds Canada Research chairs in inflammatory response signalling. O.K.M. is supported by a postdoctoral fellowship from the Société Québécoise d'Hypertension Artérielle. I.C. is a Programme de bourses de chercheur-boursier clinicien « Senior » Volet Fondamental (Fonds de la recherche en sante du Quebec) and holds a Canadian Institutes of Health Research grant (CIHR MOP 125857) that supported this work.

## References

- Kanter JE, Bornfeldt KE. Inflammation and diabetes-accelerated atherosclerosis: myeloid cell mediators. *Trends Endocrinol Metab* 2013;**24**:137-144.
- Kanter JE, Averill MM, Leboeuf RC, Bornfeldt KE. Diabetes-accelerated atherosclerosis and inflammation. *Circ Res* 2008;**103**:e116-e117.

3. Palmer AK, Tchkonja T, LeBrasseur NK, Chini EN, Xu M, Kirkland JL. Cellular senescence in type 2 diabetes: a therapeutic opportunity. *Diabetes* 2015;**64**:2289–2298.
4. Coppe JP, Desprez PY, Krtolica A, Campisi J. The senescence-associated secretory phenotype: the dark side of tumor suppression. *Annu Rev Pathol Mech Dis* 2010;**5**:99–118.
5. Salminen A, Kauppinen A, Kaarniranta K. Emerging role of NF-kappaB signaling in the induction of senescence-associated secretory phenotype (SASP). *Cell Signal* 2012;**24**:835–845.
6. Hayden MS, Ghosh S. Shared principles in NF-kappaB signaling. *Cell* 2008;**132**:344–362.
7. Solinas G, Karin M. JNK1 and IKKbeta: molecular links between obesity and metabolic dysfunction. *FASEB J* 2010;**24**:2596–2611.
8. Brand K, Page S, Rogler G, Bartsch A, Brandl R, Knuechel R, Page M, Kaltschmidt C, Baeuerle PA, Neumeier D. Activated transcription factor nuclear factor-kappa B is present in the atherosclerotic lesion. *J Clin Invest* 1996;**97**:1715–1722.
9. Park SH, Sui Y, Gizard F, Xu J, Rios-Pilier J, Hlesley RN, Han SS, Zhou C. Myeloid-specific IkkappaB kinase beta deficiency decreases atherosclerosis in low-density lipoprotein receptor-deficient mice. *Arterioscler Thromb Vasc Biol* 2012;**32**:2869–2876.
10. Liu T, Zhang L, Joo D, Sun SC. NF-kappaB signaling in inflammation. *Signal Transduct Target Ther* 2017;**2**:e17023.
11. Libby P, Everett BM. Novel antiatherosclerotic therapies. *Arterioscler Thromb Vasc Biol* 2019;**39**:538–545.
12. Ridker PM. Clinician's guide to reducing inflammation to reduce atherothrombotic risk: JACC review topic of the week. *J Am Coll Cardiol* 2018;**72**:3320–3331.
13. Atsma DE, Fibbe WE, Rabelink TJ. Opportunities and challenges for mesenchymal stem cell-mediated heart repair. *Curr Opin Lipidol* 2007;**18**:645–649.
14. Frodermann V, van Duijn J, van Pel M, van Santbrink PJ, Bot I, Kuiper J, de Jager SC. Mesenchymal stem cells reduce murine atherosclerosis development. *Sci Rep* 2015;**5**:15559.
15. Takafuji Y, Hori M, Mizuno T, Harada-Shiba M. Humoral factors secreted from adipose tissue-derived mesenchymal stem cells ameliorate atherosclerosis in Ldlr<sup>-/-</sup> mice. *Cardiovasc Res* 2019;**115**:1041–1051.
16. Miao C, Lei M, Hu W, Han S, Wang Q. A brief review: the therapeutic potential of bone marrow mesenchymal stem cells in myocardial infarction. *Stem Cell Res Ther* 2017;**8**:242.
17. Kizilay Mancini O, Lora M, Shum-Tim D, Nadeau S, Rodier F, Colmegna I. A proinflammatory secretome mediates the impaired immunopotency of human mesenchymal stromal cells in elderly patients with atherosclerosis. *Stem Cells Transl Med* 2017;**6**:1132–1140.
18. Kizilay Mancini O, Shum-Tim D, Stochaj U, Correa JA, Colmegna I. Age, atherosclerosis and type 2 diabetes reduce human mesenchymal stromal cell-mediated T-cell suppression. *Stem Cell Res Ther* 2015;**6**:140.
19. Kizilay Mancini O, Lora M, Cuillerier A, Shum-Tim D, Hamdy R, Burelle Y, Servant MJ, Stochaj U, Colmegna I. Mitochondrial oxidative stress reduces the immunopotency of mesenchymal stromal cells in adults with coronary artery disease. *Circ Res* 2018;**122**:255–266.
20. Dominici M, Le Blanc K, Mueller I, Slaper-Cortenbach I, Marini F, Krause D, Deans R, Keating A, Prockop D, Horwitz E. Minimal criteria for defining multipotent mesenchymal stromal cells. The International Society for Cellular Therapy position statement. *Cytotherapy* 2006;**8**:315–317.
21. Doyon P, van Zuylen WJ, Servant MJ. Role of IkkappaB kinase-beta in the growth-promoting effects of angiotensin II in vitro and in vivo. *Arterioscler Thromb Vasc Biol* 2013;**33**:2850–2857.
22. Dimri GP, Lee X, Basile G, Acosta M, Scott G, Roskelley C, Medrano EE, Linskens M, Rubelj I, Pereira-Smith O. A biomarker that identifies senescent human cells in culture and in aging skin in vivo. *Proc Natl Acad Sci U S A* 1995;**92**:9363–9367.
23. King KR, Aguirre AD, Ye YX, Sun Y, Roh JD, Ng RP, Jr., Kohler RH, Arlauckas SP, Iwamoto Y, Savol A, Sadreyev RI, Kelly M, Fitzgibbons TP, Fitzgerald KA, Mitchison T, Libby P, Nahrendorf M, Weissleder R. IRF3 and type I interferons fuel a fatal response to myocardial infarction. *Nat Med* 2017;**23**:1481–1487.
24. Goldin A, Beckman JA, Schmidt AM, Creager MA. Advanced glycation end products: sparking the development of diabetic vascular injury. *Circulation* 2006;**114**:597–605.
25. Lotze MT, Tracey KJ. High-mobility group box 1 protein (HMGB1): nuclear weapon in the immune arsenal. *Nat Rev Immunol* 2005;**5**:331–342.
26. Sakurai H, Chiba H, Miyoshi H, Sugita T, Toriumi W. IkkappaB kinases phosphorylate NF-kappaB p65 subunit on serine 536 in the transactivation domain. *J Biol Chem* 1999;**274**:30353–30356.
27. Bertolo A, Baur M, Guerrero J, Potzel T, Stoyanov J. Autofluorescence is a reliable in vitro marker of cellular senescence in human mesenchymal stromal cells. *Sci Rep* 2019;**9**:2074.
28. Luo JL, Kamata H, Karin M. IKK/NF-kappaB signaling: balancing life and death—a new approach to cancer therapy. *J Clin Invest* 2005;**115**:2625–2632.
29. Ley SC, Beyaert R. Priming IKKbeta kinase for action. *Biochem J* 2014;**463**:e1–e2.
30. Kamota T, Li TS, Morikage N, Murakami M, Ohshima M, Kubo M, Kobayashi T, Mikamo A, Ikeda Y, Matsuzaki M, Hamano K. Ischemic pre-conditioning enhances the mobilization and recruitment of bone marrow stem cells to protect against ischemia/reperfusion injury in the late phase. *J Am Coll Cardiol* 2009;**53**:1814–1822.
31. Shi RZ, Wang JC, Huang SH, Wang XJ, Li QP. Angiotensin II induces vascular endothelial growth factor synthesis in mesenchymal stem cells. *Exp Cell Res* 2009;**315**:10–15.
32. Perkins ND. More than just an IkkappaB kinase: the IKK complex coordinates mRNA stability and transcription. *EMBO J* 2018;**37**:e101084.
33. Qudrat A, Wong J, Truong K. Engineering mammalian cells to seek senescence-associated secretory phenotypes. *J Cell Sci* 2017;**130**:3116–3123.
34. Ritschel VN, Seljeflot I, Arnesen H, Halvorsen S, Weiss T, Eritsland J, Andersen GO. IL-6 signalling in patients with acute ST-elevation myocardial infarction. *Results Immunol* 2014;**4**:8–13.
35. Michler RE. The current status of stem cell therapy in ischemic heart disease. *J Card Surg* 2018;**33**:520–531.
36. Galipeau J, Sensebe L. Mesenchymal stromal cells: clinical challenges and therapeutic opportunities. *Cell Stem Cell* 2018;**22**:824–833.
37. Ott C, Jacobs K, Haucke E, Navarrete Santos A, Grune T, Simm A. Role of advanced glycation end products in cellular signaling. *Redox Biol* 2014;**2**:411–429.
38. Yang Y, Xia F, Hermance N, Mabb A, Simonson S, Morrissey S, Gandhi P, Munson M, Miyamoto S, Kelliher MA. A cytosolic ATM/NEMO/RIP1 complex recruits TAK1 to mediate the NF-kappaB and p38 mitogen-activated protein kinase (MAPK)/MAPK-activated protein 2 responses to DNA damage. *Mol Cell Biol* 2011;**31**:2774–2786.
39. Soro-Paavonen A, Watson AM, Li J, Paavonen K, Koitka A, Calkin AC, Barit D, Coughlan MT, Drew BG, Lancaster GI, Thomas M, Forbes JM, Nawroth PP, Bierhaus A, Cooper ME, Jandeleit-Dahm KA. Receptor for advanced glycation end products (RAGE) deficiency attenuates the development of atherosclerosis in diabetes. *Diabetes* 2008;**57**:2461–2469.
40. Yu Y, Wang L, Delguste F, Durand A, Guilbaud A, Roussel C, Schmidt AM, Tessier F, Boulanger E, Neviere R. Advanced glycation end products receptor RAGE controls myocardial dysfunction and oxidative stress in high-fat fed mice by sustaining mitochondrial dynamics and autophagy-lysosome pathway. *Free Radic Biol Med* 2017;**112**:397–410.
41. Kislinger T, Fu C, Huber B, Qu W, Taguchi A, Du Yan S, Hofmann M, Yan SF, Pischetsrieder M, Stern D, Schmidt AM. N(epsilon)-(carboxymethyl)lysine adducts of proteins are ligands for receptor for advanced glycation end products that activate cell signaling pathways and modulate gene expression. *J Biol Chem* 1999;**274**:31740–31749.
42. Lee S, Piao C, Kim G, Kim JY, Choi E, Lee M. Production and application of HMGB1 derived recombinant RAGE-antagonist peptide for anti-inflammatory therapy in acute lung injury. *Eur J Pharm Sci* 2018;**114**:275–284.
43. Audard J, Godet T, Blondonnet R, Joffredo JB, Paquette B, Belville C, Lavergne M, Gross C, Pasteur J, Bouvier D, Blanchon L, Sapin V, Pereira B, Constantin JM, Jabaudon M. Inhibition of the receptor for advanced glycation end-products in acute respiratory distress syndrome: a randomised laboratory trial in piglets. *Sci Rep* 2019;**9**:9227.
44. Creagh-Brown BC, Quinlan GJ, Evans TW, Burke-Gaffney A. The RAGE axis in systemic inflammation, acute lung injury and myocardial dysfunction: an important therapeutic target? *Intensive Care Med* 2010;**36**:1644–1656.
45. Ritschel VN, Seljeflot I, Arnesen H, Halvorsen S, Eritsland J, Fagerland MW, Andersen GO. Circulating levels of IL-6 receptor and gp130 and long-term clinical outcomes in ST-elevation myocardial infarction. *J Am Heart Assoc* 2016;**5**:e003014.
46. Anderson DR, Poterucha JT, Mikuls TR, Duryee MJ, Garvin RP, Klassen LW, Shurmur SW, Thiele GM. IL-6 and its receptors in coronary artery disease and acute myocardial infarction. *Cytokine* 2013;**62**:395–400.
47. Groot HE, Hartman MH, Gu YL, de Smet BJ, van den Heuvel AF, Lipsic E, van der Harst P. Soluble interleukin 6 receptor levels are associated with reduced myocardial reperfusion after percutaneous coronary intervention for acute myocardial infarction. *Cytokine* 2015;**73**:207–212.
48. Baldari S, Rocco DG, Piccoli M, Pozzobon M, Muraca M, Toietta G. Challenges and strategies for improving the regenerative effects of mesenchymal stromal cell-based therapies. *Int J Mol Sci* 2017;**18**:2087.

## Translational perspective

Mesenchymal stromal cells (MSCs) are potent modulators of the immune system and used in clinical trials of inflammatory conditions including atherosclerotic cardiovascular diseases. MSC-secreted bioactive molecules (i.e. secretome) mediate the crosstalk between MSCs and innate/adaptive immune cells. Further, the balance between anti- and pro-inflammatory factors in secretome determines immunopotency. We show that MSCs from diabetic patients with atherosclerosis constitutively express activated forms of the inflammatory effector IKK $\beta$  and NF- $\kappa$ B that shifts their secretome towards a pro-inflammatory phenotype and reduces their healing capacity *in vivo*. Our work emphasizes the importance of proper donor selection and the feasibility of enhancing the immunopotency of atherosclerotic+T2DM-MSC by *ex vivo* targeting IKK $\beta$ .